Soy Protein Plastics Reinforced and Toughened by SiO_2 Nanoparticles

Fujin Ai,[1] Hua Zheng,[1] Ming Wei,[1] Jin Huang[1,2]

[1]*Joint Laboratory of Polymer Modification and Functional Materials, College of Chemical Engineering, Wuhan University of Technology, Wuhan 430070, China*
[2]*Key Laboratory of Cellulose and Lignocellulosics Chemistry, Guangzhou Institute of Chemistry, Chinese Academy of Sciences, Guangzhou 510650, China*

Received 11 September 2006; accepted 20 December 2006
DOI 10.1002/app.26175
Published online 25 April 2007 in Wiley InterScience (www.interscience.wiley.com).

ABSTRACT: The nano-SiO_2 particles were compounded into soy protein isolated (SPI) matrix to produce a series of reinforcing nanocomposite sheets by compression-molding. Except for the expected increase of strength and modulus, the elongation was also enhanced when the nano-SiO_2 content was lower than 8 wt %. Moreover, two nanocomposite materials were recommended: the one is a nanocomposite containing 4 wt % nano-SiO_2 with the highest strength and enhanced elongation, the other is a reinforced material with the best elongation filled by 8 wt % nano-SiO_2. The increase of nano-SiO_2 content produced many kinds of distributions in SPI matrix, such as single nanosphere, $\sim$ 100 nm nanocluster, interconnected network structure and great domain. Such structures strongly affected the mechanical performances of nanocomposite materials. The simultaneous enhancement of strength and elongation was related to homogeneous dispersion of nanoclusters while aggregated great domains severely decreased elongation in spite of obvious reinforcing effect. However, the reinforced materials with high loading of inorganic filler should be paid attention and have economic value to some extent in practical application. With the changes of nano-SiO_2 distribution, the structures of SPI matrix changed as well. After adding a mall amount of nano-SiO_2, the damage of glycerol plasticization to ordered structure of SPI was reduced. But as nano-SiO_2 content increased, the SPI microphase was separated from nano-SiO_2 domains. Furthermore, the condition of simultaneous reinforcing and toughening was put forward: the moderate aggregation of nano-SiO_2 as well as all kinds of strong interfacial interactions. J Appl Polym Sci 105: 1597–1604, 2007

Key words: soy protein; biodegradable; nanocomposite; mechanical properties

INTRODUCTION

Nowadays, the claim of environmental protection and the lack of petroleum resource provide a new opportunity of developing the materials based on renewable natural polymers[1]. Soy protein was evaluated as a good substitute for petroleum resource because of its high rigidity and good adhesion as well as low-cost and biodegradability[2,3]. The research and application of soy protein products began in 1940[4], and recently has been rapidly developed as eco-friendly plastics and adhesive[2]. However, the preparation of soy protein plastics strongly depended on the plasticization of polyols or water to overcome brittleness and poor processability[5,6]. As a result, it was put forward how to settle the significant decrease of strength after introducing plasticizers. The blending with other biodegradable polymers was extensively accepted[7–10], while filling some rigid fillers, such as chitin[11] and its whisker[12], industrial lignin[13] and cellulose whisker[14], layered silicate[15,16] and carbon nanotube[17] and so on, showed obvious reinforcing effects.

Bionanocomposites, or econanocomposites, are novel materials based on renewable resources combined with the nanoscale effects by *in situ* assembling nanophase[10] or blending organic and inorganic nanoparticles[12,14–18]. It is just the prominent reinforcing effects and low loading of nanofiller that draw attentions to developing soy-protein based bionanocomposite[10,12,14–17]. The supramolecular nanoaggregates of hydroxylpropyl lignin can spontaneously form into SPI plastics in mixing process to enhance the strength of materials[10]. In addition, the inorganic nanostructured objects were also introduced as a good attempt. The layered silicates, montmorillonite,[15] and rectorite[16] were compounded with SPI matrix by solution mixing and melting-compression,

Correspondence to: J. Huang (huangjin@iccas.ac.cn).
Contract grant sponsor: State Key Laboratory of Pulp and Paper Engineering, South China University of Technology; contract grant number: 200514.
Contract grant sponsor: Key Laboratory of Cellulose and Lignocellulosics Chemistry, Guangzhou Institute of Chemistry, Chinese Academy of Sciences; contract grant number: LCLC-2005-172.

and then the exfoliated lamella can strongly adhere the SPI matrix by strong electrostatic affiliating as well as hydrogen bonding, resulting in an enhancement of strength. Now, other analogous attempts to modifying soy protein plastics were carried out in our groups, and the selected fillers including SiO_2 nanoparticle, carbon nanotube[17], and rhombus nanoplatelets aggregated by rod-like polyrotaxanes of cyclodextrin included polymer[19].

Herein, the nano-SiO_2 filled soy protein plastics were prepared in the process of solution mixing followed by compression-molding. Except for observing the distributions of nano-SiO_2 in SPI matrix by transmission electron microscope (TEM), the structures and mechanical properties of the molded sheets were characterized by X-ray diffraction (XRD), scanning electron microscope (SEM), differential scanning calorimetry (DSC), and tensile test. Considering the unique effects of nanometric size, high performances of complex materials are expected except for only strength increasing. On the basis of the testing results, the mechanism of enhancing mechanical performance was discussed while the structure-properties relationships were established.

EXPERIMENTAL

Materials

Commercial SPI was purchased from DuPont-Yunmeng Protein Technology Co. Ltd. (Yunmeng, China). The weight-average molecular weight (M_w) of SPI was determined by multi-angle laser light scattering instrument (MALLS, DAWN® DSP, Wyatt Technology Co., USA) equipped with a He-Ne laser ($\lambda = 632.8$ nm) to be 2.05×10^5, while the original moisture content, protein content (more than 90 wt %) and amino acid compositions (18 diverse amino acids) of SPI have been investigated and detailed in our previous paper[10]. The SiO_2 nanoprticle (nano-SiO_2) was supplied by Key Laboratory of Organsilica, Education Ministry of China (Wuhan, China). Glycerol purchased from the Shanghai Chemical Co. (Shanghai, China) was of analytical grade.

Preparation of nanocomposite sheets

10 g SPI was dissolved in 160 mL distilled water at ambient temperature with mechanical stirring to obtain an emulsion. At the same time, a desired amount of nano-SiO_2 was dispersed in 40 mL distilled water with the ultrasonic help and then mechanical stirred for 30 min. Subsequently, the nano-SiO_2 dispersion was slowly added into SPI emulsion with severe stirring for 2 h for producing a homogeneous suspension. The resultant mixing suspensions were vacuum-dried for 48 h to obtain a series of nanocomposite powders.

A series of nanocomposite powders were mechanically mixed with the plasticizer of glycerol respectively; the weight ratio of every solid powder and glycerol was controlled as 70 : 30 all the time. Subsequently, the glycerol plasticized powders were compression-molded as the sheets at 140°C under the pressure of 20 MPa for 5 min, and then air-cooled to 50°C for half-hour before releasing the pressure for demolding. The dimension of the obtained sheets with the thickness of $\sim$ 0.50 mm was about 70 mm $\times$70 mm. According to the nano-SiO_2 content in original freeze-dried powders, the molded sheets were coded as the S-nSi-0, S-nSi-4, S-nSi-8, S-nSi-12, S-nSi-16, S-nSi-20 and S-nSi-24, respectively. The nanocomposite sheets were conditioned in a desiccator with silica gel desiccant for one week at room temperature before characterization.

Characterization

X-ray diffraction (XRD) patterns were performed on a D/max-2500 X-ray diffractometer (Rigaku Denki, Japan) with Cu Kα_1 radiation ($\lambda = 0.154$ nm) in a rang of $2\theta = 3$–60° using a fixed time mode with a step interval of 0.02°. Additionally, the crystalline degree (χ_c) was calculated by the accessory software of instrument.

Scanning electron microscope (SEM) was carried out on a Hitachi X-650 scanning electron microscope. The sheets were frozen in liquid nitrogen and then snapped immediately. The fracture surfaces (the cross sections) of the films were sputtered with gold and then observed and photographed. Transmittance electron microscope (TEM) was performed with a FEI TecnaiG2 20 electron microscope at 180 kV. The ultrathin sections of the nanocomposite sheets were prepared by using a diamond knife on a Leica Ultracut UCT with EMFCS cryo-attachment at −120°C. The ultrathin sections with cross section thickness of 60 nm were directly placed on the copper grids for observation and photographing.

DSC analysis was carried out on a DSC-204 instrument (Netzsch, Germany) under nitrogen atmosphere at a heating or cooling rate of 20°C min^{-1}. The sheets were scanned in the range of −150 to 100°C after a pretreatment (heating from 20 to 100°C and then cooling down to −150 °C) of eliminating the thermal history.

The tensile strength (σ_b), elongation at break (ε_b), and Young's modulus (E) of the nanocomposite sheets were measured on a universal testing machine (CMT6503, Shenzhen SANS Test Machine Co. Ltd., Shenzhen, China) with a tensile rate of 5 mm min^{-1} according to ISO527-3:1995(E). The tested samples were cut into the quadrate strips with the width of

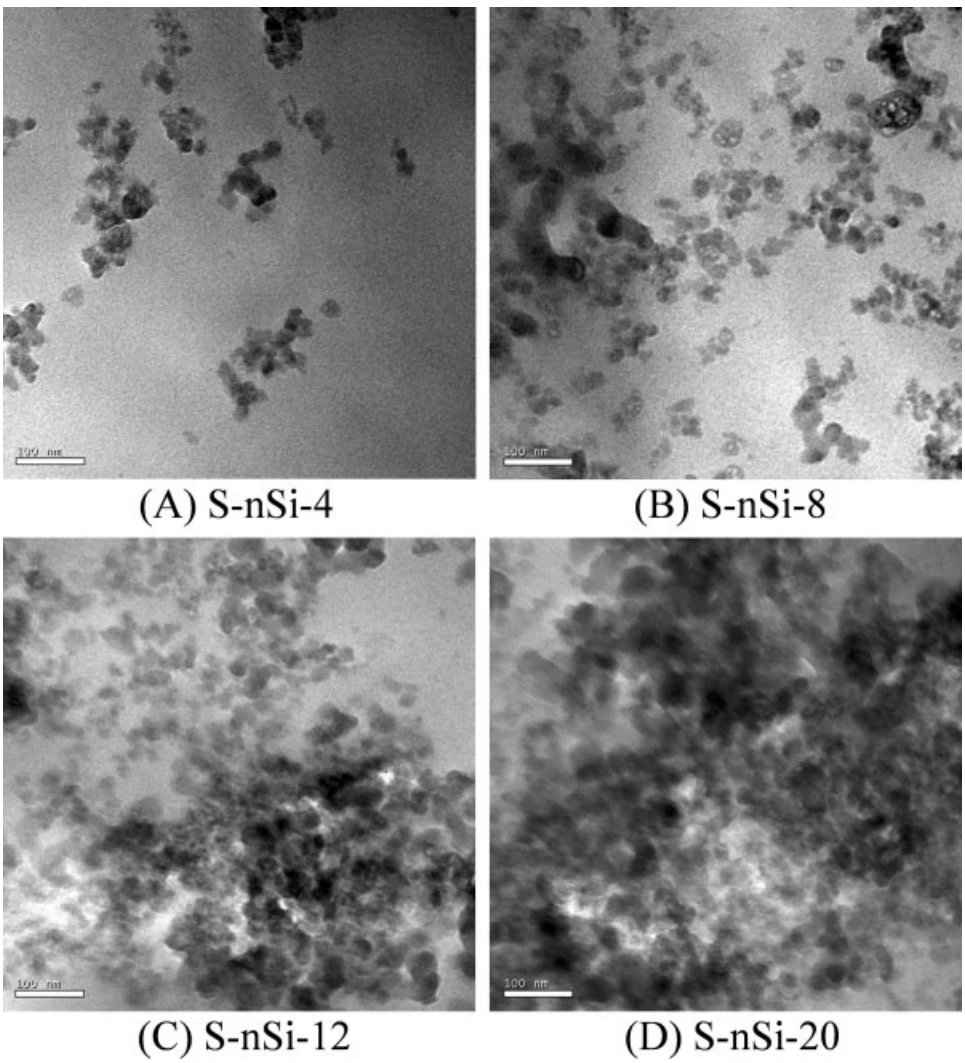

Figure 1 TEM images of the ultrathin sections from compression-molding nanocomposite sheets with the nano-SiO_2 contents of 4 wt % (A, S-nSi-4), 8 wt % (B, S-nSi-8), 12 wt % (C, S-nSi-12) and 20 wt % (D, S-nSi-20).

10 mm, and the distance between testing marks was 40 mm. The tested strips were kept in the humidity of 35% for 7 days before measurement. An average value of five replicates of each sample was taken.

RESULTS AND DISCUSSION

Distributions of nano-SiO_2 in SPI matrix

TEM images in Figure 1 clearly visualized the sizes and distributions of nano-SiO_2 and their aggregates in SPI matrix. As shown in Figure 1(A) of S-nSi-4, the SiO_2 nanospheres were little isolated and tended to aggregate as the clusters with about 100 nm. The formation of nanoclusters suggested that the interaction among SiO_2 nanoparticles was stronger than that at the interface of nano-SiO_2 and SPI. As the adding content of nano-SiO_2 increased up to 8 wt %, Figure 1(B) of S-nSi-8 showed that the nano-SiO_2 uniformly dispersed in SPI matrix became more while more nanospheres individually existed as well as aggregated nanoclusters. With a continuous increase of nano-SiO_2 content, the nano-SiO_2 clusters were interconnected to form network-like structure and aggregated as dense domains, shown by Figure 1(C) of S-nSi-12. Additionally, too high nano-SiO_2 content resulted in a large area of adjacent aggregated domains, and the example was shown as Figure 1(D) of S-nSi-20.

As a result, it can be summarized that the aggregation of nano-SiO_2 is predominant driven by stronger interaction among nanoparticles. With increasing nano-SiO_2 content, the initial aggregated nanoclusters could be interconnected as network-like structure and then further aggregate to great domains. Such three typical structures with different scale as well as various interactions at nano-SiO_2/nano-SiO_2 interface, at nano-SiO_2/SPI matrix interface and in

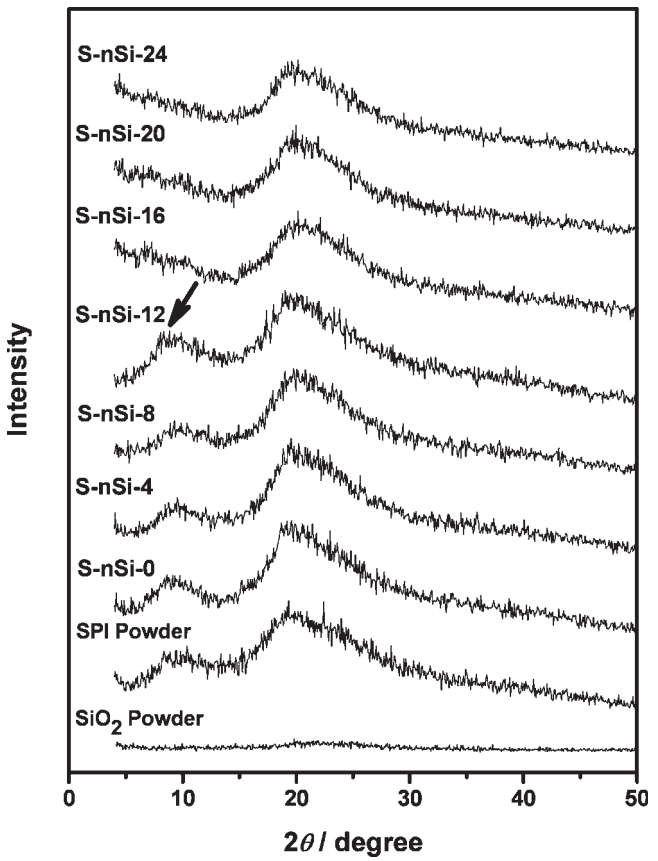

Figure 2 XRD patterns of the compression-molding nanocomposite sheets from the freeze-dried powders with different nano-SiO_2 contents as well as SPI and nano-SiO_2 powders.

SPI matrix would directly cause the changes of original structure in SPI matrix and hence affect mechanical performance of nanocomposites.

Structural changes after adding nano-SiO_2

The XRD pattern in Figure 2 suggested that there existed some ordered structure in SPI powder, i.e., crystalline domains, shown as two peaks located at about 8.8 and 19.0° as well as the crystalline degree (χ_c) of 16.62%. The glycerol-plasticized SPI sheet (S-nSi-0) inherited the semicrystalline character of SPI powder and had a slightly low χ_c value of 16.40%. It indicated that the ordered structure was slightly destroyed in plasticizing and melting process because the SPI molecules motion and become stretching. Firstly, the XRD patterns of nanocomposite sheets with low loading of nano-SiO_2 were similar to S-nSi-0 without nano-SiO_2. However, when the adding content of nano-SiO_2 was higher than 12 wt %, the peak located at 8.8° disappeared, indicating that the long-range ordered structure in SPI matrix was destroyed. Combined with TEM images, such damage resulted from the formation of highly aggregated great domains. Although adding amorphous nano-SiO_2 normally resulted in a decrease of crystalline degree, the decrease tendency was not linear. Figure 3 showed the effects of nano-SiO_2 content on χ_c value as well as the hypothetic linear change shown as a dash line, which obtained from the linear connection from 16.40% of χ_c for pure SPI plasticized sheet to 0% of χ_c for amorphous nano-SiO_2. It was worth of note that the positive deviation occurred until the nano-SiO_2 content of 12 wt % and thereafter the negative deviation did. Interestedly, this transition was just agreement with the disappearance for the peak at 8.8°. As a result, it was deduced that the negative derivation of χ_c resulted from the damage of long-range ordered structure. Additionally, the positive deviation suggested that the dispersed SiO_2 nanoclusters restricted the motion of SPI molecules driven by glycerol as plasticizer in melting process, and hence kept the original ordered structure in SPI powder.

The glass transition originated from the relaxation motion of polymer chains at the molecular level from glassy state to rubbery state; it can reflect the differences of chemical environments in composite materials, such as intermolecular interaction, spatial hindrance and so on. Herein, some sheets with or without nano-SiO_2 were measured by DSC, and the

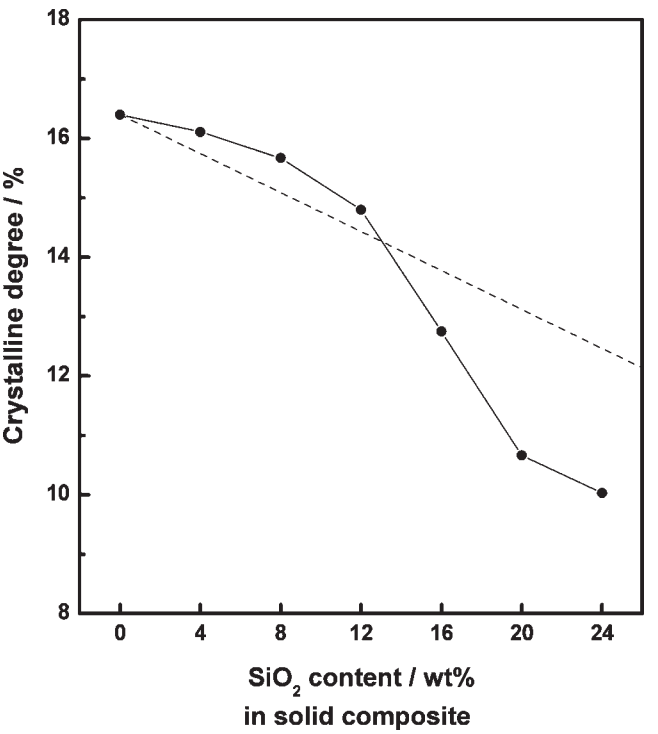

Figure 3 Effects of nano-SiO_2 content on the crystalline degree (χ_c) of nanocomposite sheets as well as pure SPI sheet. (The dash line was the linear connection from 16.40% of χ_c for pure SPI sheet to 0% of χ_c for amorphous nano-SiO_2.)

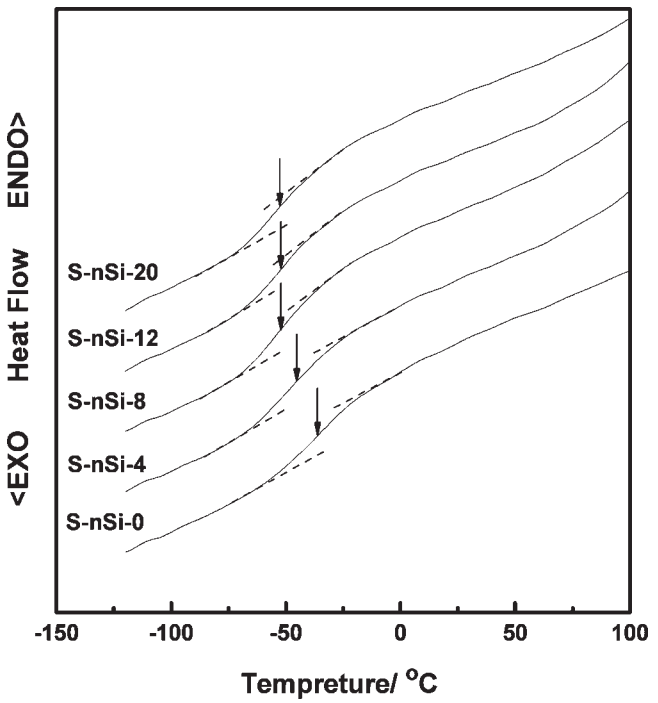

Figure 4 DSC thermograms of the nanocomposite sheets containing 4 wt % (S-nSi-4), 8 wt % (S-nSi-8), 12 wt % (S-nSi-12), and 20 wt % (S-nSi-20) nano-SiO_2 as well as the pure SPI sheet (S-nSi-0).

thermograms and data of glass transition temperature (T_g) and heat-capacity increment (ΔC_p) were depicted in Figure 4 and Table I respectively. Obviously, the addition of nano-SiO_2 caused an increase of weight ratio of glycerol to SPI, which made the SPI chains motion more easily and decreased the glass transition temperature. However, the decrease of glass transition temperature was not proportioned with the adding content of nano-SiO_2. After the server decrease for *S*-nSi-4, the $T_{g,\text{onset}}$ and $T_{g,\text{mid}}$ continuously decreased up to *S*-nSi-8 with increasing nano-SiO_2 content, and then slightly increased for *S*-nSi-12. It suggested that the motion of SPI molecules was restricted by added nano-SiO_2. Additionally, the lowest $T_{g,\text{onset}}$ and $T_{g,\text{mid}}$ of *S*-nSi-20 caused by the severer microphase separation between nano-SiO_2 great domains and SPI matrix. If only considering that the weight ratio of glycerol to SPI increased with increasing nano-SiO_2 content, the ΔC_p should gradually decrease and lower than that of S-nSi-0. However, the results showed an enhanced ΔC_p for the nanocomposite sheets with nano-SiO_2 of lower than 8 wt %. It attributed to the strong interaction at the interface of nano-objects and SPI matrix while the uniform dispersion at small nanoscale was also a key factor. As the aggregated great domains appeared, the contact area of nano-objects to SPI matrix reduced in spite of the increase of nano-SiO_2, resulting in the lowest ΔC_p for S-nSi-12. Thereafter, as the nano-SiO_2 unceasingly increased, the ΔC_p of S-nSi-20 increased, but lower than pure SPI sheet (S-nSi-0) as well. The T_g ranges, codetermined by $T_{g,\text{onset}}$ and $T_{g,\text{end}}$, for the sheets containing nano-SiO_2 were narrower than that of S-nSi-0 without nano-SiO_2, suggesting that the structure of SPI component became homogeneous, i.e., the original structure of SPI component was partly destroyed. Combined with the XRD results, the destroyed structure of SPI matrix mentioned here was not the ordered structure except for S-nSi-20, but should involve amorphous domain and others.

As a whole, the addition of nano-SiO_2 would destroy the original structure of SPI matrix. However, the extent and region of destroy in SPI matrix was functioned as the adding content of nano-SiO_2. A small amount of nano-SiO_2 (lower than 12 wt %) favored keeping the long-range ordered structure of SPI matrix by restricting the motion of SPI molecules with strong interfacial interaction between nano-objects and SPI matrix. In addition, the microphase sparation between SPI matrix and nano-SiO_2 great domains occurred when the nano-SiO_2 content was higher than 12 wt %.

Cryo-fractured behavior of nanocomposite sheets

The SEM images of fractured surface for nanocomposite sheets and S-nSi-0 without adding nano-SiO_2 were shown in Figure 5. Similar to previous report[10], S-nSi-0 only containing SPI showed a heterogeneous morphology [Figure 5(A)] originated from the complex component and structure in soy protein, such as globin domain, crystalline domain, amorphous domain and so on. Such fractured morphology did

TABLE I
Glass Transition Temperature (T_g) at Onset, Mid and End Point, T_g Range, and Heat-Capacity Increment (ΔC_p) for the Sheets with and without Nano-SiO_2 Determined by DSC

Sample	$T_{g,\text{onst}}$ (°C)	$T_{g,\text{mid}}$ (°C)	$T_{g,\text{end}}$ (°C)	T_g range (°C)	ΔC_p (J g^{-1} K^{-1})
S-nSi-0	−59.3	−36.6	−13.8	45.5	0.641
S-nSi-4	−68.5	−46.7	−24.9	43.6	0.654
S-nSi-8	−70.8	−51.1	−31.5	39.3	0.653
S-nSi-12	−69.3	−51.0	−32.6	36.7	0.601
S-nSi-20	−71.5	−51.3	−31.2	40.3	0.624

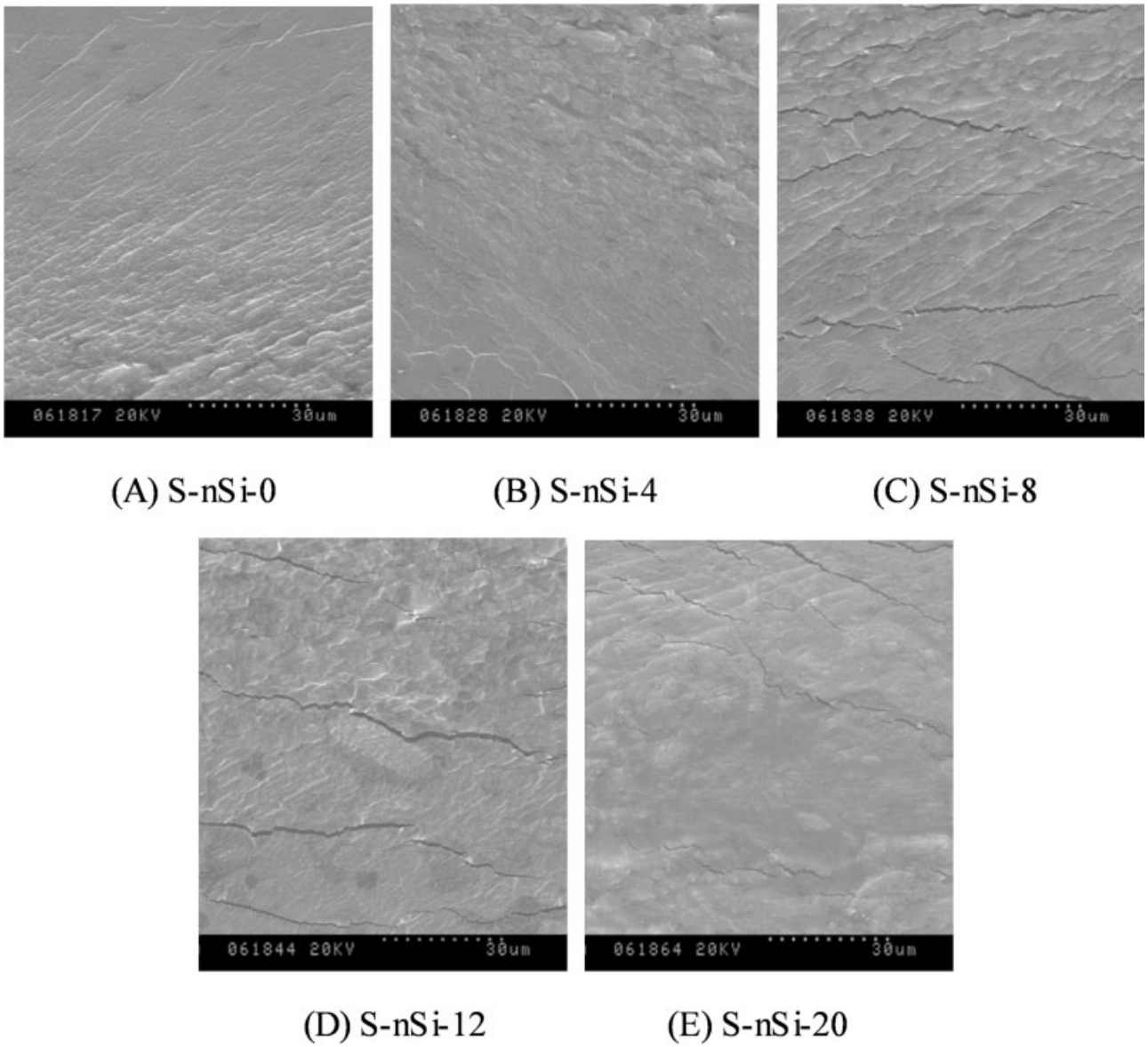

Figure 5 SEM images of the fractured surfaces for compression-molding sheets without nano-SiO_2 (A, S-nSi-0) and with the nano-SiO_2 of 4 wt % (B, S-nSi-4), 8 wt % (C, S-nSi-8), 12 wt % (D, S-nSi-12), and 20 wt % (E, S-nSi-20).

not obviously changed after adding 4 wt % nano-SiO_2 because only a small number of nanoclusters with about 100 nm well dispersed in to SPI matrix (shown by TEM image) and the original structure of SPI matrix was destroyed very weakly especially for the observation at large scale. However, the obvious change of fractured surface after adding nano-SiO_2 can be observed as a more coarse structure for S-nSi-8 because the fraction of nanoclusters and individual SiO_2 nanospheres increased and also kept homogeneous dispersion in SPI matrix. As the nano-SiO_2 gradually interconnected to form network and aggregated as great domains due to the unceasing increase of nano-SiO_2 content, the fluctuant structure was replaced by the fractured surface with some smooth regions. The smooth region may result from the removing of aggregated nano-SiO_2 after cryo-fracturing, indicating a brittle-fractured character.

When 4 wt % nano-SiO_2 was added, the original structure of SPI matrix was mostly kept and the interfacial adhesion between nanoclusters and SPI matrix might favor enhancing the strength, modulus and even elongation. The fractured surface of S-nSi-8 sheet was most heterogeneous, indicating there existed more intermolecular association among components. Such structure forecasted higher elongation as well as enhanced strength. As regards to the nanocomposite sheets with high nano-SiO_2 content (more than 12 wt %), the brittle-fractured character became more and more obvious. Although the mod-

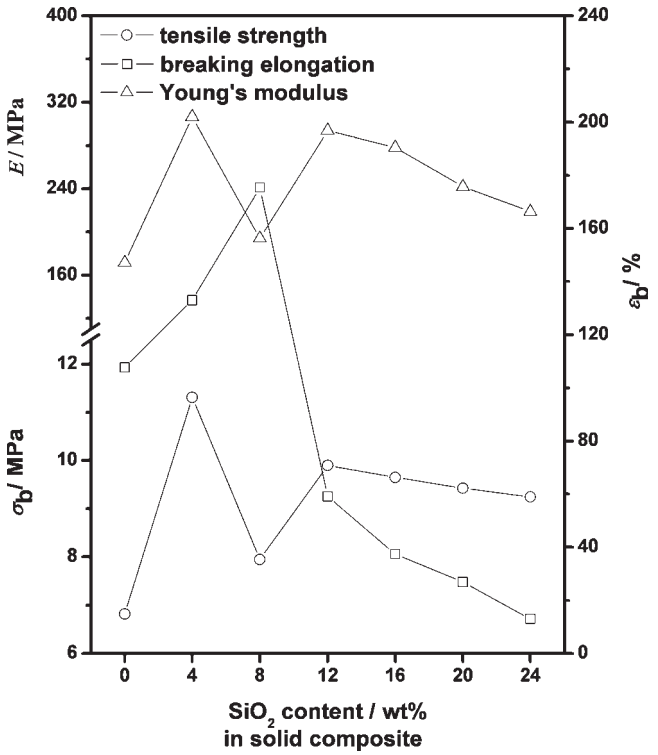

Figure 6 Effects of nano-SiO_2 contents on tensile strength (σ_b), elongation at break (ε_b) and Young's modulus (E) for the nanocomposite sheets as well as the reference of the S-nSi-0 sheet without adding nano-SiO_2.

ulus, i.e., rigidity, of nanocomposite sheet can be confirmed, the decrease of elongation was inevitable and hence damaged the strength of materials.

Mechanical properties of nanocomposite sheets

Figure 6 showed the effects of nano-SiO_2 contents on the mechanical properties of *S*-nSi nanocomposite sheet, including tensile strength (σ_b), Young's modulus (E) and elongation at break (ε_b). The effects of nano-SiO_2 content on σ_b and E were similar: both maximum values happened as adding 4 wt % nano-SiO_2 followed by a sharp decrease for S-nSi-8; thereafter, σ_b and E increased up to S-nSi-12 and then slightly decrease with increasing nano-SiO_2 content. In any case, introducing nano-SiO_2 realized a prominent reinforcing effect. Except for expected strength increase, the elongation was also obviously enhanced for the sheets with nano-SiO_2 content lower than 8 wt %. The elongation at break firstly increased from 108% (S-nSi-0 without nano-SiO_2) to 175% (S-nSi-8 containing 8 wt % nano-SiO_2), and then sharply decreased up to 59% with the addition of 12 wt % nano-SiO_2 followed by a slight decrease as the nano-SiO_2 content increased unceasingly. It is worth noting that the maximum strength of 11.3 MPa happened at the addition of 4wt% nano-SiO_2 with an enhancement of elongation, and that adding 8 wt % nano-SiO_2 resulted in optimal elongation as well as a reinforcing effect.

The changes of mechanical performance were well consistent with the hypothesis from cyro-fractured morphology combined with other test results. Firstly, the strong interaction at the interface between SPI matrix and nano-SiO_2 was the guarantee of enhancing mechanical performances. Furthermore, the uniformly dispersed nanoclusters and individual nanospheres became the stress concentrated points and hence increased the strength. In addition, more associations among components, shown by a heterogeneous fractured surface for S-nSi-8 [Fig. 5(C)], favored highest elongation. The sharply decrease of elongation for the sheets containing nano-SiO_2 of higher than 12 wt % as well as the decrease of strength resulted from the formation of great domains and induced microphase separation even though the continuous network in the S-nSi-12 sheet favored enhancing mechanical performances. Except for emphasizing the role of nano-SiO_2, the structural changes of SPI matrix should be also considered. Although a small amount of nano-SiO_2 destroyed the original structure of SPI weakly, it restricted the damage of glycerol plasticization to ordered structure, showing a positive derivation of χ_c. It confirmed the enhancement of strength on the other hand. However, too high loading would boost the destroy of the original structure in SPI matrix and induce the microphase separation between components, resulting in a decrease of mechanical performances.

Mechanism of reinforcement and toughening

There are three kinds of interaction contributing to the strength existed in this kind of nanocomposite materials, such as original interaction in SPI matrix, the interfacial interaction between SPI matrix and nano-SiO_2, and the self-aggregated affinity among nano-SiO_2 (Scheme 1). Usually, the excess self-aggregation of nano-objects can damage the function of nanometer scale. Herein, the nano-SiO_2 inevitably self-aggregated as nanoclusters and even great domains as well. However, it was fortunate that the aggregated clusters lied in nanoscale and all nano-objects homogeneously dispersed when the nano-SiO_2 content was lower than 8 wt %, which provided more contact area between SPI matrix and nanoparticles and hence produced stronger interfacial adhesion. In addition to keeping the rigid crystalline domains in SPI matrix, the reinforcing of materials necessarily happened. It is easily accepted that the interaction between nanparticles was strongest while the interfacial interaction between SPI and nanoparticles was stronger than the interaction in SPI matrix.

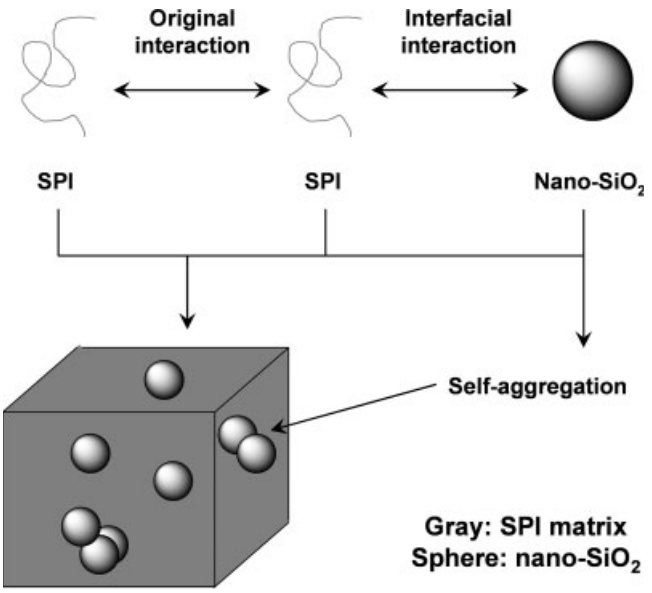

Scheme 1 Schematic illustration for the various interactions in nanocomposite material as well as the distribution of nano-SiO_2 in SPI matrix.

Because the stress can transfer at all kinds of interfaces while all interfacial interactions are lower than covalent bonds, the interface with strongest adhesion would determine the strength of complex materials. As a result, the S-nSi-8 sheet had the lowest reinforcing effect due to more individually dispersed nanospheres; herein, the strength of complex materials was dominated by the interface at nano-SiO_2/SPI with mediate interaction. The simultaneous increase of elongation was mainly related to the structural character in nanocomposites besides the interaction basis. In the nanocomposit sheets with the nano-SiO_2 content of lower than 8 wt %, nano-SiO_2 aggregated as unshaped clusters with about 100 nm. In the tensile process, the interconnected nanoparticles in clusters would gradually arrange along the tensile direction until the sheet broke, which favored the enhancement of the elongation.

CONCLUSIONS

The rigid nano-SiO_2 particles were compounded into soy protein isolated (SPI) matrix to produce a kind of reinforced and toughened nanocomposite materials, i.e., the strength, modulus and elongation were simultaneously enhanced when the nano-SiO_2 content was lower than 8 wt %. The improvement of mechanical performance mainly attributed to homogeneous dispersion of nanoclusters as well as all kinds of strong interfacial interactions. Additionally, it also played an important role that a small amount of nano-SiO_2 not only kept the ordered structure in SPI matrix by restricting the damage of glycerol plasticization. Although high loading would benefit higher economic value and have reinforcing function as well, the sharply decrease of elongation was a big pity all the time. At this time, nano-SiO_2 self-aggregated as great domains, showing obvious microphase separation from SPI matrix in nanocomposite materials. Although such nanocomposite materials herein is far way from practical application, the predominant mechanical performance impulses the development of soy protein plastics beyond all doubt. In addition, the simultaneous reinforcing and toughening effect might submit a strategy of material design.

The authors are grateful to Dr. Ronghua Huang (Wuhan University) for the supply of SiO_2 nanoparticles, and Mr. Kun Zhang (Zhongshan University) for the help of DSC measurement.

References

1. Chiellini, E.; Cinelli, P.; Chiellini, F.; Imam, S. H. Macromol Biosci 2004, 4, 218.
2. Kumar, R.; Choudhary, V.; Mishra, S.; Varma, I. K.; Mattiason, B. Ind Crop Prod 2002, 16, 155.
3. Sue, H. J.; Wang, S.; Jane, J. Polymer 1997, 38, 5035.
4. Brother, G. H.; McKinney, L. L. Ind Eng Chem 1940, 32, 1002.
5. Wang, S.; Sue, H. J.; Jane, J. J Macromol Sci Pure Appl Chem 1996, A33, 557.
6. Chen, P.; Zhang, L. Acromol Biosci 2005, 5, 237.
7. Zhang, J.; Jiang, L.; Zhu, L.; Jane, J.; Mungara, P. Biomacromolecules 2006, 7, 1551.
8. Zhang, J.; Mungara, P.; Jane, J. Polymer 2001, 42, 2569.
9. Huang, J.; Zhang, L.; Chen, F. J Appl Polym Sci 2003, 88, 3284.
10. Wei, M.; Fan, L.; Huang, J.; Chen, Y. Macromol Mater Eng 2006, 291, 524.
11. Zheng, H.; Tan, Z.; Zhan, Y.; Huang, J. J Appl Polym Sci 2003, 90, 3676.
12. Lu, Y.; Weng, L.; Zhang, L. Biomacromolecules 2004, 5, 1046.
13. Huang, J.; Zhang, L.; Chen, P. J Appl Polym Sci 2003, 88, 3291.
14. Wang, Y.; Cao, X.; Zhang, L. Macromol Biosci 2006, 6, 524.
15. Chen, P.; Zhang, L. Biomacromolecules 2006, 7, 1700.
16. Yu, J.; Cui, G.; Wei, M.; Huang, J. J Appl Polym Sci, to appear.
17. Zheng, H.; Ai, F.; Wei, M.; Huang, J. Macromol Mater Eng, submitted.
18. Angellier, H.; Molina-Boisseau, S.; Dole, P.; Dufresne, A. Biomacromolecules 2006, 7, 531.
19. Zheng, H.; Zhou, Z.; Wei, M.; Huang, J. Macromol Biosci, submitted.